View metadata, citation and similar papers at core.ac.uk
brought to you by CORE
provided by RERO DOC Digital Library

Int J Cardiovasc Imaging (2014) 30:1399–1405
DOI 10.1007/s10554-014-0474-0

ORIGINAL PAPER

Coronary artery calcium quantification from contrast enhanced CT using gemstone spectral imaging and material decomposition

Tobias A. Fuchs · Julia Stehli · Svetlana Dougoud · Bert-Ram Sah · Sacha Bull · Olivier F. Clerc · Mathias Possner · Ronny R. Buechel · Oliver Gaemperli · Philipp A. Kaufmann

Received: 26 March 2014 / Accepted: 16 June 2014 / Published online: 4 July 2014
© Springer Science+Business Media Dordrecht 2014

Abstract To explore the feasibility of coronary artery calcium (CAC) measurement from low-dose contrast enhanced coronary CT angiography (CCTA) as this may obviate the need for an unenhanced CT scan. 52 patients underwent unenhanced cardiac CT and prospectively ECG triggered contrast enhanced CCTA (Discovery HD 750, GE Healthcare, Milwaukee, WI, USA). The latter was acquired in single-source dual-energy mode [gemstone spectral imaging (GSI)]. Virtual unenhanced images were generated from GSI CCTA by monochromatic image reconstruction of 70 keV allowing selective iodine material suppression. CAC scores from virtual unenhanced CT were compared to standard unenhanced CT including a linear regression model. After iodine subtraction from the contrast enhanced CCTA the attenuation in the ascending aorta decreased significantly from 359 ± 61 to 54 ± 8 HU ($P < 0.001$), the latter comparing well to the value of 64 ± 55 HU found in the standard unenhanced CT ($P =$ ns) confirming successful iodine subtraction. After introducing linear regression formula the mean values for Agatston, Volume and Mass scores of virtual unenhanced CT were 187 ± 321, 72 ± 114 mm^3, and 27 ± 46 mg/cm^3, comparing well to the values from standard unenhanced CT (187 ± 309, 72 ± 110 mm^3, and 27 ± 45 mg/cm^3) yielding an excellent correlation ($r = 0.96$, $r = 0.96$, $r = 0.92$; $P < 0.001$). Mean estimated radiation dose revealed 0.83 ± 0.02 mSv from the unenhanced CT and 1.70 ± 0.53 mSv from the contrast enhanced CCTA. Single-source dual-energy scanning with GSI allows CAC quantification from low dose contrast enhanced CCTA by virtual iodine contrast subtraction.

Keywords Coronary CT angiography · Calcium scoring · Single-source dual energy

Introduction

Coronary computed tomography angiography (CCTA) is an established non-invasive tool for evaluation of coronary artery disease (CAD) in daily clinical routine yielding high accuracy compared to invasive coronary angiography [1–3]. The CCTA is often preceded by an unenhanced CT for coronary artery calcification (CAC) assessment. The prognostic value of CAC score has been well established [4]. On the other hand a high value of CAC scoring is often associated with increasing numbers of non-diagnostic segments in CCTA. Therefore, it is generally accepted, that in patients with pronounced CAC values a CCTA may be deferred to avoid non-diagnostic CCTA [5], but no clear cut threshold for this decision has been established and therefore the current guidelines leave this to the discretion of the physician [6]. As a consequence although the combination of CAC and CCTA has been shown to provide added diagnostic and prognostic value [7–9], a substantial number of patients with coronary calcifications will not undergo both scans. This is mainly due to radiation protection issues, urging that a scan with reduced diagnostic accuracy should be avoided. In order to offer the benefit of both CCTA and CAC assessment to patients referred to cardiac CT evaluation without the need of an unenhanced

Tobias A. Fuchs and Julia Stehli have contributed equally to this work.

T. A. Fuchs · J. Stehli · S. Dougoud · B.-R. Sah · S. Bull · O. F. Clerc · M. Possner · R. R. Buechel · O. Gaemperli · P. A. Kaufmann (✉)
Cardiac Imaging, Nuclear Medicine, University Hospital Zurich, Ramistrasse 100, NUK C 42, 8091 Zurich, Switzerland
e-mail: pak@usz.ch

CT scan, several studies have investigated the feasibility of CAC assessment from contrast enhanced CCTA [10] but mostly failed to provide a method with satisfactory results suitable for clinical use in daily practice.

Recently, by use of dual-energy based virtual non-contrast CT CAC values with good correlation to unenhanced CT were obtained [11]. However, only calcium volume values were assessed albeit not the Agatston score, although the latter is the most established and most widely used in daily clinical routine. Furthermore the protocol resulted in a radiation dose exposure of 15 mSv despite ECG triggered tube modulation.

Recently a new single-source dual-energy CCTA technology, the gemstone spectral imaging (GSI) has been introduced combining fast kVp switching (dynamic switching between two different energy levels of X-rays from one source) with latest gemstone detectors allowing generation of monochromatic images and suppression of known materials such as iodine. As a result, images with iodine suppression allow synthesizing virtually unenhanced images from which CAC may be assessed.

The aim of the present pilot study was to explore the feasibility of CAC measurement by use of images obtained from contrast enhanced low-dose CCTA as this may obviate the need for an unenhanced CT scan.

Methods

Study population

The study population consisted of 52 patients, who were referred to prospectively triggered contrast-enhanced CCTA scanning for assessment of known or suspected CAD, who additionally underwent unenhanced cardiac CT for CAC scoring and attenuation correction of nuclear myocardial perfusion imaging [12–14]. All scans were clinically indicated and the need for written informed consent was waived by the institutional review board (local ethics committee) due to the retrospective nature of this study with sole clinical data collection. Patients with stents, pacemaker leads, prior coronary bypass graft surgery, and motion artifacts were excluded.

CT data acquisition and reconstruction

All CT scans were performed on a high definition CT scanner (Discovery HD 750, GE Healthcare, Milwaukee, WI, USA). Unenhanced CT scans for CAC measurements covering the whole heart were performed previously ($n = 32$) or after ($n = 20$) contrast enhanced CCTA, using prospectively ECG-triggered sequential images as previously reported in detail [15]. Briefly, unenhanced CT images were obtained during inspiration breath hold using the following parameters: detector coverage 40 mm, slice thickness 2.5 mm, gantry rotation time 0.35 s, temporal resolution 0.175 s, tube voltage of 120 kV and tube current of 200 mA. Prospectively ECG-triggered contrast-enhanced CCTA [16] was acquired with the smallest default beam window (zero additional padding) during inspiration breath hold using GSI, that includes a X-ray source, which can switch energy between 80 and 140 kVp within 0.3–0.5 ms and is complemented by a gemstone detector with very fast primary speed and low afterglow time. Metoprolol (up to 25 mg Beloc, AtraZeneca, London, UK) was administered intravenously prior to the examination if the heart rate was higher than 65 beats per minute in order to obtain optimal image quality for CCTA. Prior to the scan 2.5 mg isosorbiddinitrate (Isoket, Schwarz Pharma, Monheim, Germany) were administered sublingually. Iodixanol (Visipaque 320, 320 mg/ml, GE Healthcare, Buckinghamshire, UK) was injected into an antecubital vein followed by 50 ml saline solution via an 18-gauge catheter. Contrast media volume (65.7 ± 17.3 ml) and flow rate (4.4 ± 0.5 ml/s) were adapted to body surface area as previously validated [17]. For contrast enhanced CCTA the following scanning parameters were used: GSI mode with fast tube voltage switching between 80 and 140 kVp on adjacent views during a single rotation; axial scan mode with 64×0.625 mm, gantry rotation time of 0.35 s and temporal resolution of 0.175 s. Tube current and mean voltage (resulting from variable switching between 80 and 140 kVp) were adapted to individual body mass index (using GSI presets offered by the vendor) as previously reported [18].

Conventional polychromatic images and synthesized monochromatic images at 70 keV with the attached GSI data file were reconstructed and transferred to a dedicated workstation (AW 4.6 GE Healthcare, Milwaukee, WI, USA) for further analysis. This includes generation of material suppressed images for iodine subtraction (CardIQ, GE Healthcare, Milwaukee, WI, USA).

CT data evaluation

A circled region of interest (ROI) was placed in the ascending aorta in all 3 datasets, e.g. in unenhanced CT, in contrast enhanced conventional polychromatic CCTA and in virtual unenhanced CT to measure mean attenuation in Hounsfield Units (HU). In order to assure that exactly the same regions were measured in different scans, the ROIs were automatically copied by the software using the scout scans as landmark.

The standard unenhanced CT and the virtual unenhanced CT were used for calcium quantification (Fig. 1). All CAC datasets were analyzed in random order using the commercially available software package (“Smartscore”,

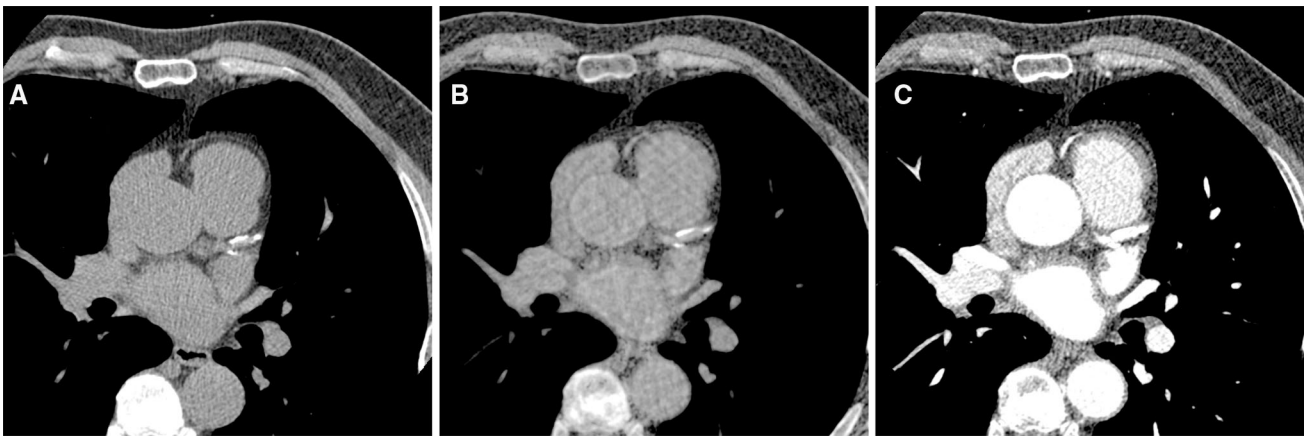

Fig. 1 Transaxial cardiac slices of standard unenhanced (**A**) and virtual unenhanced CT (**B**) both with window width 240 HU and window center 40 HU. The latter is synthesized by suppression of iodine from contrast enhanced CCTA (**C**)

GE Healthcare, Milwaukee, USA). For analysis of unenhanced CT scan the DICOM header of the contrast enhanced CCTA was adjusted to allow analysis in this software package. The Agatston, the Volume and the Mass score were obtained from each CT scan as previously reported [19] according to recommendations for standardization from the International Consortium of Standardization in Cardiac CT [20] and reported as the summed total CAC value. Values for Agatston score were also given as age and gender stratified percentiles [21].

Effective radiation dose from each scan was calculated as the product of dose-length product times a conversion coefficient for chest (k = 0.014 mSv/(mGy × cm)) [22].

Statistical analysis

The statistical software package SPSS 20.0 (SPSS, Chicago, IL) was used for analysis. Quantitative variables were expressed as mean ± standard deviation (SD) and categorical variables as frequencies or percentages. The data were tested for normal distribution by using Shapiro–Wilk test. Comparison of variables were performed with Mann–Whitney U. A linear regression model was performed for CAC values from unenhanced versus virtual unenhanced datasets. As a result the regression models for CAC values revealed Agatston = 0.224 × Agatston (virtual) − 5.602, Mass = 0.385 × Mass (virtual) − 1.073 and Volume = 0.546 × Volume (virtual) − 6.064. The formula obtained from the latter was then applied to the Hounsfield values obtained from virtual unenhanced CT scans to correct for the errors introduced by transformation form polychromatic to monochromatic datasets. Correlations between CAC values from unenhanced and virtual unenhanced series were expressed as Spearman correlation coefficients (r) and Bland–Altman (BA) limits of agreement [23] were calculated for uncorrected and the corrected data. *P* values of less than 0.05 were considered statistically significant.

Table 1 Patient characteristics ($n = 52$)

Characteristic	Value
Age (mean ± SD, years)	62 ± 8
Male (%)	46
BMI (mean ± SD, kg/m^2)	27 ± 5
Cardiovascular risk factors	
Diabetes (%)	10
Dyslipidemia (%)	50
Hypertension (%)	60
Positive family history (%)	50
Smoking (%)	38

SD standard deviation, *BMI* body mass index

Results

Patients had an average age of 62 ± 8 years and a mean body mass index of 27 ± 5 kg/m^2 (Table 1). The estimation of the radiation dose revealed mean values of 0.83 ± 0.02 mSv from the unenhanced CT and 1.70 ± 0.53 mSv from the contrast enhanced CCTA. The standard unenhanced CT scan revealed mean values for Agatston, Volume and Mass of 187 ± 309, 72 ± 110 mm^3, and 27 ± 45 mg/cm^3.

After iodine subtraction from the contrast enhanced CCTA the mean attenuation in the ascending aorta decreased significantly from 359 ± 61 to 54 ± 8 HU ($P < 0.001$), in the virtual unenhanced CT, the latter comparing well to the mean value of 64 ± 55 HU found in the standard unenhanced CT confirming successful iodine subtraction (P = ns, Fig. 2). The mean values from the

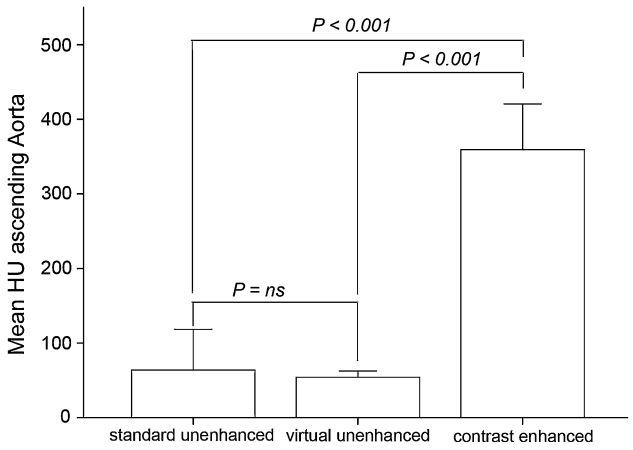

Fig. 2 After iodine subtraction from the contrast enhanced CCTA the mean attenuation averaged from each ascending aorta (n = 52) decreased significantly from 359 ± 61 to 54 ± 8 HU ($P < 0.001$), comparing well to the 64 ± 55 HU found in the unenhanced CT (P = ns). This confirms successful iodine subtraction by material decomposition

virtual unenhanced CT for Agatston, Volume and Mass scores were 36 ± 72, 33 ± 62 mm^3, and 9 ± 18 mg/cm^3, respectively. After introducing the formula obtained from the linear regression analysis the mean values for Agatston, Volume and Mass scores were 187 ± 321, 72 ± 114 mm^3, and 27 ± 46 mg/cm^3, comparing well to the values from unenhanced CT. In true unenhanced CT 12 patients had a CAC of 0, all 12 patients had a CAC of 0 concordant in virtual unenhanced CT confirming the successful comprehensive subtraction of the entire iodine.

There was an excellent correlation of the values obtained from the unenhanced and the virtual unenhanced CT for Agatston (r = 0.96, $P < 0.001$), Volume (r = 0.96, $P < 0.001$), and Mass (r = 0.92, $P < 0.001$). The BA limits of agreement, however, were −621 to +320 for Agatston, −142 to +64 mm^3 for Volume, and −73 to +37 mg/cm^3 for Mass, respectively. After introducing the formula obtained from the linear regression analysis the BA limits of agreements further improved for Agatston (−174 to +174), Volume (−55 to +55 mm^3), and Mass (−19 to +19 mg/cm^3), respectively (Fig. 3).

The agreement between virtual unenhanced and true unenhanced CT scan to detect a CAC score of 0 was 90 %. The agreement between the two methods to detect an age and gender stratified CAC score >75th Agatston percentile was 94 %.

Discussion

The present results support that single-source dual-energy scanning with GSI allows CAC quantification for low dose contrast enhanced CCTA by virtual iodine contrast subtraction. The very fast kV tube switch of the present single source scanner allows acquisition of complementary datasets at different energy levels, which is required to differentiate material, particularly with high anatomic numbers such as iodine. The processed material suppression algorithm proved successful in subtracting iodine, as the results of CAC quantification from the virtual unenhanced images revealed an excellent correlation for Agatston, Volume, and Mass values with the true unenhanced CT scoring as standard of reference. This holds particularly true when using the derived linear regression formula, which allows adjusting the virtual material subtraction values to the values from standard unenhanced scanning. These adjustments represent the necessary calibration taking into account the characteristics of the scanner, including the properties of fast kVp switching and its specific impact on the gemstone semiconductor detectors. Our results are the first to document that with the described single-source dual-energy technique accurate CAC quantification is feasible from contrast enhanced low-dose CCTA without the need for an additional unenhanced CT scan. This may decrease the total study acquisition time, cost, and radiation to the patient. The prognostic value of CAC scoring has been widely documented [4]. Furthermore its added prognostic and diagnostic value when used in combination with CCTA has been previously established [7, 8]. Therefore, it has become common practice to precede CCTA with an unenhanced cardiac CT scan for CAC quantification. It has been shown that a more extensive CAC reflects a higher likelihood for the presence of obstructive coronary lesions [24, 25]. On the other hand, it is well known that the greater the extend of CAC, the greater the probability that coronary evaluation for exact luminal narrowing assessment will be non-diagnostic in calcified segments [26]. Therefore, some centers use the extent of CAC to guide the next step of the cardiac protocol as they do not proceed with a CCTA if the unenhanced CT reveals a CAC score exceeding 600–1,000. However, such approaches still lack adequate evaluation and are therefore not endorsed by current guidelines [6]. In fact, the latter clearly state that in selected patients CCTA may yield useful information despite extensive CAC.

The introduction of the present method would allow assessing CAC from CCTA, combining the benefits of both pieces of information. This can be achieved with a low radiation dose CCTA by material suppression imaging, which is based on a novel single-source dual-energy approach whereby the beam is switched during two-thirds of the time to a lower voltage of 80 kVp, while during only one-third it is switched to 140 kVp. In combination with prospectively triggering and a minimized beam time duration (minimal window with zero additional padding)

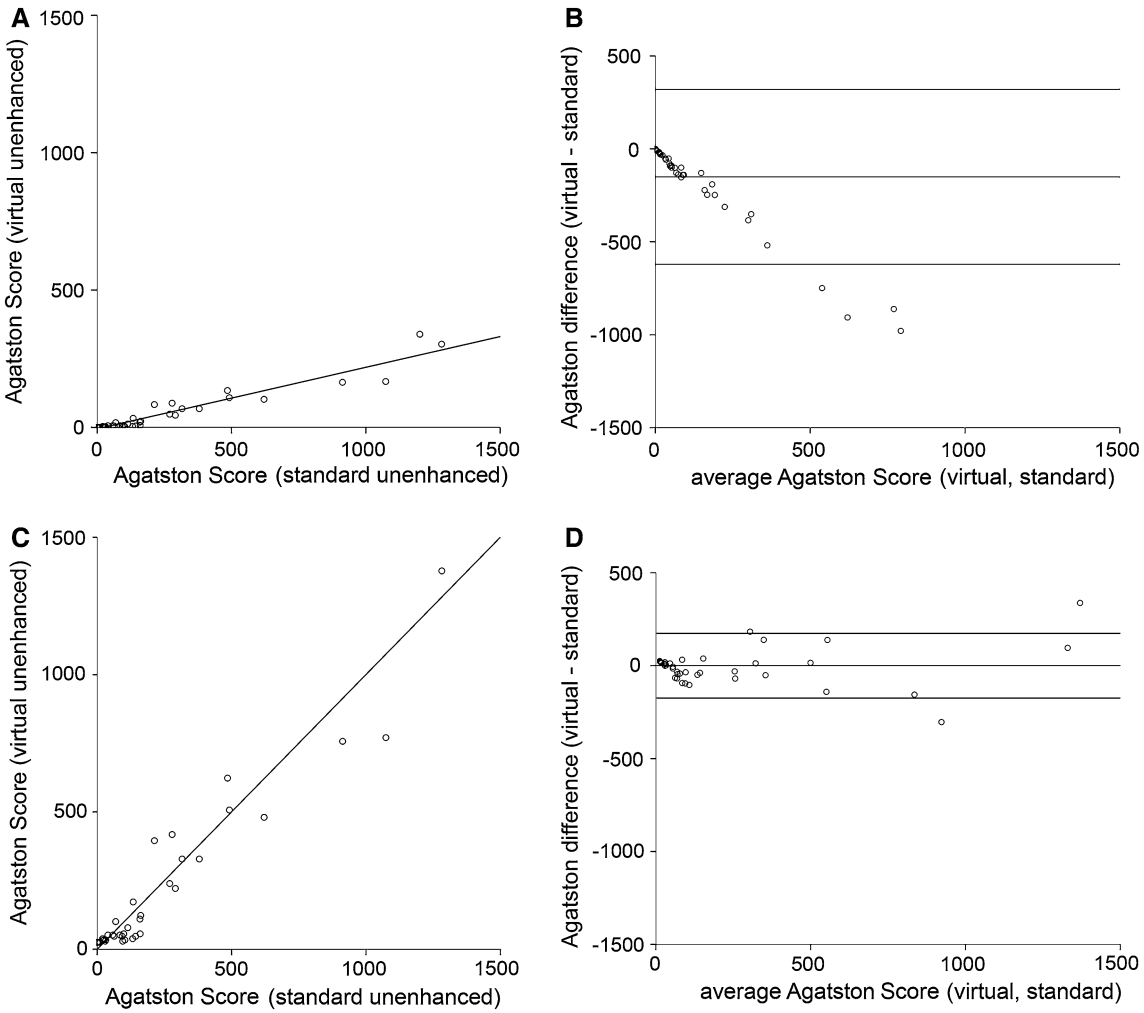

Fig. 3 There was an excellent correlation ($r = 0.96$, $P < 0.001$) between Agatston values from standard unenhanced versus virtual unenhanced scans (**A**), with relatively large Bland–Altman limits of agreement (**B**). After introducing the correction formula derived from the linear regression analysis the values were closer to the line of unity (**C**) and the limits of agreement substantially more narrow (**D**). The remaining gaps between the limits may be further closed by more refined calibration factors and more advanced algorithms

[27] this results in a mean radiation dose estimation of 1.7 ± 0.5 mSv, which is substantially lower than the previously reported 15.8 ± 3.8 mSv [11].

Limitations

A limitation of the present study is the fact that despite excellent correlation between CAC values from the virtual unenhanced and the standard enhanced scan the BA limits of agreement remain relatively wide. How far apart measurements can be without causing a problem remains a question of clinical judgment for each individual patient and setting. Nevertheless, it appears desirable to achieve more narrow limits of agreement for CAC measurements from virtual unenhanced CT. This, however, requires further evaluation because the standards established for CAC quantification [20] are based on HU obtained in polychromatic unenhanced scans, and may not apply to 70 keV reconstructions as HU differ significantly in monochromatic scans according to the energy chosen for reconstruction. Thus, the excellent correlation of CAC values from virtual versus standard unenhanced CT scans found in our study provides the ground on which the use of virtual unenhanced CT scanning for CAC may be based in the future while the necessary calibration factors yet await to be established. In fact, the CAC values obtained from virtual unenhanced CT were underestimated without correction. This indicates that discrimination of iodine from calcification is not yet perfect with an overlay causing partial subtraction of CAC, due to misinterpretation as iodine.

The applicability of such an algorithm established for calculating the Agatston score from the CCTA is presumably confined to the scanner type and model used in the

present study and may be different for other devices. This, however, holds true for all calibration factors which need to be established for each scanner before CAC measurement in standard unenhanced CT, because the calibration factors are scanner specific. Finally, the present study did not include phantoms as standard of reference. However, the use of patients reflecting all challenges of daily clinical routine seemed more appropriate than phantoms, particularly as each patient served as his/her own control. In addition, Agatston values are calculated with an algorithm but do not represent a physical gold standard making calibration against any phantom elusive.

Conclusion

In conclusion, our results suggest that single-source dual-energy scanning with GSI allows CAC quantification from low dose contrast enhanced CCTA by virtual iodine contrast subtraction.

Acknowledgments The study was supported by grants from the Swiss National Science Foundation (SNSF) to PAK. Furthermore, we thank our cardiac radiographers Ennio Mueller and Gentian Cermjani for their excellent technical support.

Conflict of interest None.

References

1. Schroeder S, Achenbach S, Bengel F, Burgstahler C, Cademartiri F, de Feyter P et al (2008) Cardiac computed tomography: indications, applications, limitations, and training requirements: report of a Writing Group deployed by the Working Group Nuclear Cardiology and Cardiac CT of the European Society of Cardiology and the European Council of Nuclear Cardiology. Eur Heart J 29(4):531–556
2. Papaefthymiou H, Athanasopoulos D, Papatheodorou G, Iatrou M, Geraga M, Christodoulou D et al (2013) Uranium and other natural radionuclides in the sediments of a Mediterranean fjord-like embayment, Amvrakikos Gulf (Ionian Sea), Greece. J Environ Radioact 122:43–54
3. Uehara M, Takaoka H, Kobayashi Y, Funabashi N (2013) Diagnostic accuracy of 320-slice computed-tomography for detection of significant coronary artery stenosis in patients with various heart rates and heart rhythms compared with conventional coronary-angiography. Int J Cardiol 167(3):809–815
4. Budoff MJ, Shaw LJ, Liu ST, Weinstein SR, Mosler TP, Tseng PH et al (2007) Long-term prognosis associated with coronary calcification: observations from a registry of 25,253 patients. J Am Coll Cardiol 49(18):1860–1870
5. Miller JM, Rochitte CE, Dewey M, Arbab-Zadeh A, Niinuma H, Gottlieb I et al (2008) Diagnostic performance of coronary angiography by 64-row CT. N Engl J Med 359(22):2324–2336
6. Abbara S, Arbab-Zadeh A, Callister TQ, Desai MY, Mamuya W, Thomson L et al (2009) SCCT guidelines for performance of coronary computed tomographic angiography: a report of the Society of Cardiovascular Computed Tomography Guidelines Committee. J Cardiovasc Comput Tomogr 3(3):190–204
7. Leschka S, Scheffel H, Desbiolles L, Plass A, Gaemperli O, Stolzmann P et al (2008) Combining dual-source computed tomography coronary angiography and calcium scoring: added value for the assessment of coronary artery disease. Heart 94(9):1154–1161
8. van Werkhoven JM, Schuijf JD, Gaemperli O, Jukema JW, Kroft LJ, Boersma E et al (2009) Incremental prognostic value of multi-slice computed tomography coronary angiography over coronary artery calcium scoring in patients with suspected coronary artery disease. Eur Heart J 30(21):2622–2629
9. Versteylen MO, Joosen IA, Winkens MH, Laufer EM, Snijder RJ, Wildberger JE et al (2013) Combined use of exercise electrocardiography, coronary calcium score and cardiac CT angiography for the prediction of major cardiovascular events in patients presenting with stable chest pain. Int J Cardiol 167(1):121–125
10. Ebersberger U, Eilot D, Goldenberg R, Lev A, Spears JR, Rowe GW et al (2013) Fully automated derivation of coronary artery calcium scores and cardiovascular risk assessment from contrast medium-enhanced coronary CT angiography studies. Eur Radiol 23(3):650–657
11. Schwarz F, Nance JW Jr, Ruzsics B, Bastarrika G, Sterzik A, Schoepf UJ (2012) Quantification of coronary artery calcium on the basis of dual-energy coronary CT angiography. Radiology 264(3):700–707
12. Schepis T, Gaemperli O, Koepfli P, Namdar M, Valenta I, Scheffel H et al (2007) Added value of coronary artery calcium score as an adjunct to gated SPECT for the evaluation of coronary artery disease in an intermediate-risk population. J Nucl Med 48(9):1424–1430
13. Schepis T, Gaemperli O, Koepfli P, Ruegg C, Burger C, Leschka S et al (2007) Use of coronary calcium score scans from stand-alone multislice computed tomography for attenuation correction of myocardial perfusion SPECT. Eur J Nucl Med Mol Imaging 34(1):11–19
14. Burkhard N, Herzog BA, Husmann L, Pazhenkottil AP, Burger IA, Buechel RR et al (2010) Coronary calcium score scans for attenuation correction of quantitative PET/CT 13N-ammonia myocardial perfusion imaging. Eur J Nucl Med Mol Imaging 37(3):517–521
15. Ghadri JR, Pazhenkottil AP, Nkoulou RN, Goetti R, Buechel RR, Husmann L et al (2011) Very high coronary calcium score unmasks obstructive coronary artery disease in patients with normal SPECT MPI. Heart 97(12):998–1003
16. Husmann L, Herzog BA, Gaemperli O, Tatsugami F, Burkhard N, Valenta I et al (2009) Diagnostic accuracy of computed tomography coronary angiography and evaluation of stress-only single-photon emission computed tomography/computed tomography hybrid imaging: comparison of prospective electrocardiogram-triggering vs. retrospective gating. Eur Heart J 30(5):600–607
17. Pazhenkottil AP, Husmann L, Buechel RR, Herzog BA, Nkoulou R, Burger IA et al (2010) Validation of a new contrast material protocol adapted to body surface area for optimized low-dose CT coronary angiography with prospective ECG-triggering. Int J Cardiovasc Imaging 26(5):591–597
18. Fuchs TA, Stehli J, Fiechter M, Dougoud S, Sah BR, Gebhard C et al (2013) First in vivo head-to-head comparison of high-definition versus standard-definition stent imaging with 64-slice computed tomography. Int J Cardiovasc Imaging 29(6):1409–1416
19. Ghadri JR, Goetti R, Fiechter M, Pazhenkottil AP, Kuest SM, Nkoulou RN et al (2011) Inter-scan variability of coronary artery calcium scoring assessed on 64-multidetector computed tomography vs. dual-source computed tomography: a head-to-head comparison. Eur Heart J 32(15):1865–1874
20. McCollough CH, Ulzheimer S, Halliburton SS, Shanneik K, White RD, Kalender WA (2007) Coronary artery calcium: a

multi-institutional, multimanufacturer international standard for quantification at cardiac CT. Radiology 243(2):527–538
21. Hoff JA, Chomka EV, Krainik AJ, Daviglus M, Rich S, Kondos GT (2001) Age and gender distributions of coronary artery calcium detected by electron beam tomography in 35,246 adults. Am J Cardiol 87(12):1335–1339
22. Ghadri JR, Kuest SM, Goetti R, Fiechter M, Pazhenkottil AP, Nkoulou RN et al (2012) Image quality and radiation dose comparison of prospectively triggered low-dose CCTA: 128-slice dual-source high-pitch spiral versus 64-slice single-source sequential acquisition. Int J Cardiovasc Imaging 28(5): 1217–1225
23. Bland JM, Altman DG (1986) Statistical methods for assessing agreement between two methods of clinical measurement. Lancet 1(8476):307–310
24. Otaki Y, Arsanjani R, Gransar H, Cheng VY, Dey D, Labounty T et al (2012) What have we learned from CONFIRM? Prognostic implications from a prospective multicenter international observational cohort study of consecutive patients undergoing coronary computed tomographic angiography. J Nucl Cardiol 19(4):787–795
25. Bajraktari G, Nicoll R, Ibrahimi P, Jashari F, Schmermund A, Henein MY (2013) Coronary calcium score correlates with estimate of total plaque burden. Int J Cardiol 167(3):1050–1052
26. Pundziute G, Schuijf JD, Jukema JW, Lamb HJ, de Roos A, van der Wall EE et al (2007) Impact of coronary calcium score on diagnostic accuracy of multislice computed tomography coronary angiography for detection of coronary artery disease. J Nucl Cardiol 14(1):36–43
27. Husmann L, Herzog BA, Burger IA, Buechel RR, Pazhenkottil AP, von Schulthess P et al (2010) Usefulness of additional coronary calcium scoring in low-dose CT coronary angiography with prospective ECG-triggering impact on total effective radiation dose and diagnostic accuracy. Acad Radiol 17(2):201–206